29th International Symposium on Shock Waves, Madison, WI July 14-19, 2013.

Reflected Detonation Waves: Comparing Theory to Measured Reflected Shock Speed

J. Damazo[1] **and J.E. Shepherd**[1]

1 Introduction

Gaseous detonations are self-sustaining shock waves propagating in combustible mixtures that are coupled to and sustained by exothermic chemical reaction [1]. These supersonic combustion events produce substantial increases in mixture pressure and temperature. Detonations also induce a velocity in the fluid through which they propagate. When a detonation impinges upon a wall, the moving fluid must be impulsively stagnated by a reflected shock wave that travels away from the wall back into the detonated gas [2]. Hence in regions near a reflecting end wall, the pressure and temperature will be increased twice in quick succession–first by the detonation and second by the reflected shock–thereby making regions near surfaces of reflection particularly important when examining how detonations effect destruction.

A space–time diagram of one-dimensional detonation propagation and normal reflection is shown in Figure 1. The detonation propagates at the Chapman–Jouguet detonation speed [1] into the unburned reactants at initial state 1 and raises the pressure and temperature to the post-detonation values at state 2. A nonsteady expansion wave (the Taylor–Zel'dovich or TZ wave) develops behind the detonation; this lowers the pressure and temperature to the final values at state 3. When the detonation impinges upon an end wall at $x = L$, a reflected shock is created to promptly stagnate the fluid behind the detonation. A model for this reflected shock was proposed in our previous study [3] and, although substantial agreement was obtained between experimental results and finite element simulations using this wave reflection model, the discrepancies in predicted shock strength suggested that not all of the appropriate physics were being captured. The present work is focused on employing high resolution pressure measurements with high-speed schlieren visualization to better understand the detonation reflection process.

California Institute of Technology, 1200 E California Blvd Pasadena, CA

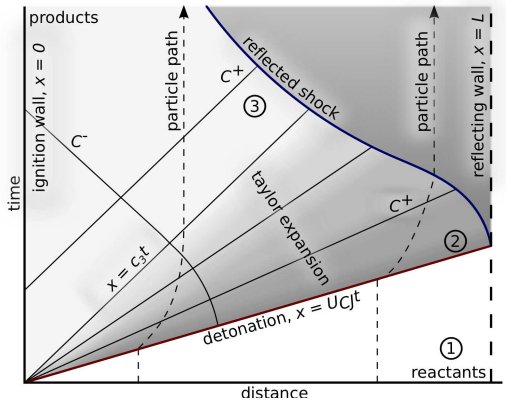

Fig. 1 Space–time diagram depicting ideal one-dimensional detonation propagation at constant speed U_{CJ} and subsequent reflection off an end-wall located at $x = L$

2 Experimental Setup

The goals of the detonation tube experiments are to measure the pressure loading created by a reflecting detonation wave. Experiments were performed in the GALCIT Detonation Tube (GDT) shown in Figure 2. The GDT is a 7.6 m long, 280 mm inner diameter detonation tube equipped with a 150 mm wide test section and two quartz windows to provide optical access. The tube was initially evacuated and then filled via the method of partial pressures to the desired composition. Detonations were initiated with an acetylene–oxygen injection system [4]. A range of conditions will be discussed in the presentation, but the results discussed herein are restricted to an test mixture of stoichiometric hydrogen–oxygen at initial pressure 25 kPa. A set of representative conditions is given in Table 1.

After ignition, a detonation enters the test section shown in the inset of Figure 2 [5]. A splitter plate was constructed to raise the floor into the center of the windows so that shock wave boundary layer interaction may be observed, if present. This splitter plate was instrumented with twelve PCB 113B26 pressure transducers. Gauge locations are given on relevant plots. Schlieren photographs such as shown in Figure 3 were obtained by employing a PL1000DRC flash lamp in combination with a SIMD16 camera in a Z–type schlieren setup [6] to obtain sixteen schlieren images at essentially arbitrary frame-rate with 20 ns exposure time. All images show the corner formed by the reflecting end wall and the floor of the splitter plate as presented in the inset to Figure 2.

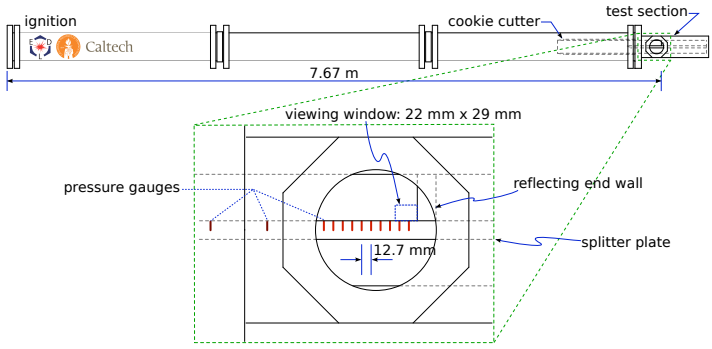

Fig. 2 An overview of the experimental facility and inset showing details of test section

3 Discussion

The experiment conditions discussed herein correspond to shots 2152 and 2179 in Table 1. The initial composition was stoichiometric hydrogen–oxygen at initial pressure $p_1 = 25$ kPa. Figure 3 displays sixteen schlieren images shown chronologically in left-to-right, top-to-bottom giving a short movie of the incident detonation and shock reflection process for shot 2152. Each frame shows the same 29 mm wide field of view. The detonation is initially seen to propagate towards the end-wall located at the right-edge of the frame. The detonation impinges upon this wall in frame 7. Frames 8–16 then show the reflected shock wave propagating back to the left. There is a great deal of information regarding the gas dynamics of detonation reflection that can be learned from these images. Focusing the analysis on the wave location in each image, we can complement the pressure measurement arrival data given below in Figure 4(a). Processing the data in each frame, we are able to determine the wave location and quantify the uncertainty due to the smearing of the front location because of the three-dimensional cellular structure of the detonation.

Figure 4(a) shows pressure signals from shots 2152 and 2179. These shots had identical initial conditions and data from both are included to illustrate the repeatability in the experiment. These pressure signals allow us to properly assess the pressure loading to the tube wall as a function of time and distance from reflection. We are also able to examine the wave time-of-arrival at each location and thereby determine wave speeds. Time-of-arrival data with a range associated with the rise time of the pressure signals is plotted for each pressure signal in Figure 4(a) as vertical dashed black lines. We see that the characterization of the arrival time range as a range is especially important for the reflected shock due to the observed rise time that is approximately 10 times longer than the rise time associated with the incident detonation. Combining this data with the arrival data obtained from the schlieren images, we can construct the space-time diagram with error bars shown in Figure 4(b). Detonation arrival data are shown in red and reflected shock arrival data are shown in blue. The dashed lines correspond to a one-dimensional zero-thickness reaction

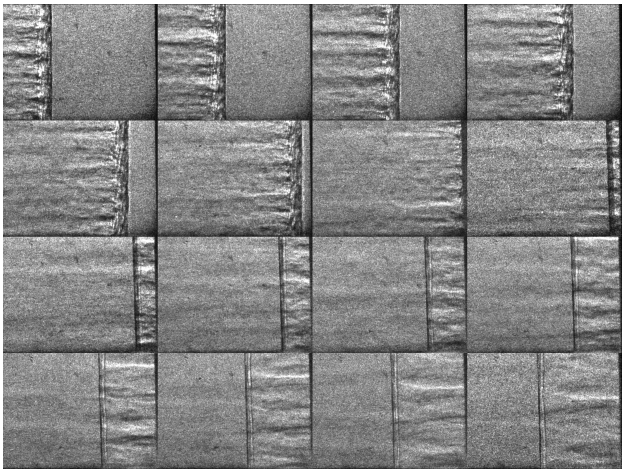

Fig. 3 Sixteen schlieren images of detonation and reflected shock propagation. The images are read left-to-right, top-to-bottom to form a 16-frame movie of the reflection event. The bottom of each image is the floor of the splitter plate and the right-hand edge of each image is the reflecting wall shown in Figure 2. The field of view was 29 mm wide by 22 mm tall and the frame-rate was 787402 frames per second

zone model [3]. The solid lines correspond to a polynomial fit to the arrival data of the form

$$X_{det} = U_{det}\,(t_0 - t) \tag{1}$$

$$X_{ref} = U_{ref}\,(t - t_0) + \frac{1}{2} a_{ref}\,(t - t_0)^2 \tag{2}$$

where X_{det} and X_{ref} are the detonation and shock locations as a function of time. U_{det} and t_0 are fit to the detonation time of arrival data and U_{ref} and a_{ref} are fit to the shock time of arrival data. Values for U_{ref} are given in Table 1.

Examining Figure 4(b), we observe that the reflected wave speed is substantially under-predicted near the wall by the zero-thickness reaction zone model. This is true in every experiment we performed and the discrepancy is far outside any measurement uncertainty. After considering various possibilities, we believe that the source of this discrepancy is that the model does not consider the finite-thickness reaction zone structure of the detonation wave. The ideal model of reflection considers a detonation of zero thickness, appearing to be a sharp jump in properties from reactants directly to combustion products. Real detonation waves consist of a non-reacting shock wave followed by a finite-thickness reaction zone. In addition, as observed in Figure 3, the detonation wave is not precisely planar and the flow behind the wave is three-dimensional due to the instability of the detonation wave as manifested by the transverse shock waves (commonly referred to as cellular structure). Setting aside the three-dimensional structure of the wave (which can only be addressed through numerical simulation), we consider the classic ZND detonation model where the

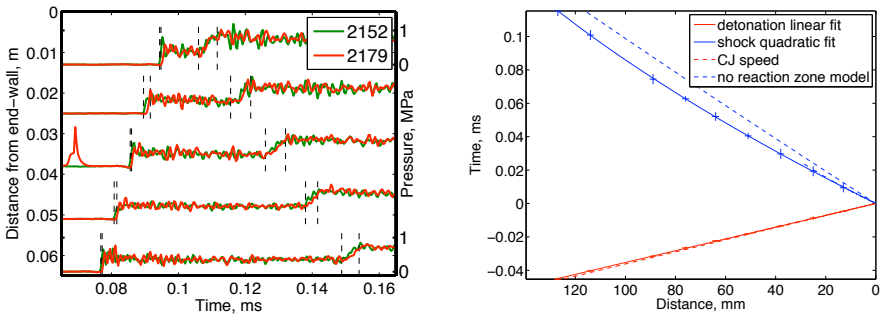

(a) (b)

Fig. 4 (**a**) Pressure data for two detonation experiments of stoichiometric H_2–O_2 at initial pressure 25 kPa. Extracted time of arrival data (*vertical dashed lines*) give a minimum and maximum for wave arrival corresponding to the signal rise times. (**b**) Time of arrival data with error bars as extracted from experimental data alongside the polynomial fit and zero reaction zone thickness model

wave is a non-reacting shock followed by a zone of chemical reaction. The rates of chemical reaction and energy release determine the structure and thickness of the reaction zone. The initial portion of the reaction zone is termed the induction zone and is a region where radicals are increasing exponentially in concentration but the energy release is small so that the thermal properties of the gas are those behind the initial non-reacting shock. At the downstream end of the induction zone, there is a narrow zone of large energy release followed by a slow approach to equilibrium.

Considering the reflection of the finite-thickness model of the detonation, we observe that immediately after the leading shock reflects from the wall it will encounter shocked but un-reacted gas. Chemical reactions will occur very quickly behind the reflected shock because the temperature and pressure are already high within the reaction zone and are increased further by the reflected shock. As a consequence the entire induction zone explodes almost instantaneously when the reflected shock moves into it. Approximating the explosion process as a detonation in the induction zone, we obtain an estimate of the initial reflected shock speed that is in better agreement with measured values. The reacting shock speed is calculated by

$$U_{ref,rxn} = U_{CJ@VN} - u_2 \tag{3}$$

where $U_{CJ@VN}$ is the Chapman–Jouguet speed for a gas initially at the von Neumann conditions behind the detonation front and u_2 is the fluid velocity behind the detonation; both of these are computed with the Shock and Detonation Toolbox [7]. In Table 1 we observe agreement to within 5% for the run conditions at initial pressure 10 and 25 kPa. When the initial pressure is 50 kPa, the shock speed is over predicted by 17% compared to a 14% under-prediction by the zero reaction zone model. This is most likely attributed to the thinner reaction zone for the higher pressure case (values for the induction length, l_{ind} are given in Table 1) leading to the post-shock combustion having a smaller effect than predicted.

Table 1 Measured and computed reflected shock speeds created by a detonation of stoichiometric hydrogen–oxygen at the listed initial pressure. U_{ref} are the measured speeds, U_{norxn} is the reflected shock speed predicted by the zero thickness reaction zone model [3], $U_{ref,rxn}$ is the speed predicted by the reacting shock model, and l_{ind} is the induction zone length

shot number	p_1 (kPa)	U_{ref} (m/s)	$U_{ref,norxn}$ (m/s)	$U_{ref,rxn}$ (m/s)	l_{ind} (μm)
2163	10	1425 ± 13	1020 ± 1	1352	510
2152	25	1389 ± 6	1040 ± 3	1393	178
2179	25	1417 ± 21	1040 ± 3	1393	178
2180	50	1219 ± 15	1055 ± 2	1425	83

4 Conclusion

Experimental results on the reflection of gaseous detonation waves are presented with a focus on the speed of the reflected shock for times near detonation reflection. It is shown that the reflected shock speed for times soon after reflection is better predicted when using a model that incorporates the finite-reaction zone thickness behind the detonation. The lower the pressure and therefore the thicker the reaction zone, the better the agreement with the present modeling approach.

Acknowledgements

This research is sponsored by the DHS through the University of Rhode Island, Center of Excellence for Explosives Detection. The authors would also like to thank Frank Kosel and Specialised Imaging for remarkable cooperation and flexibility regarding the use of the SIMD16 camera, which is truly an exceptional machine.

References

1. Fickett, W. and Davis, W. C., *Detonation*, University of California Press, Berkerely, CA, 1979.
2. Shepherd, J., Teodorcyzk, A., Knystautas, R., and Lee, J., "Shock Waves Produced by Reflected Detonations," *Progress in Astronautics and Aeronautics*, Vol. 134, 1991, pp. 244–264.
3. Karnesky, J., Damazo, J., Chow-Yee, K., Rusinek, A., and Shepherd, J., "Plastic deformation due to reflected detonation," *International Journal of Solids and Structures*, Vol. 50, No. 1, 2013, pp. 97–110.
4. Akbar, R., *Mach Reflection of Gaseous Detonations*, PhD dissertation, Rensselaer Polytechnic Institute, 1997.
5. Kaneshige, M. J., *Gaseous Detonation Initiation and Stabilization by Hypervelocity Projectiles*, PhD dissertation, California Institute of Technology, 1999.
6. Settles, G. S., *Schlieren and Shadowgraph Techniques*, Springer-Verlag Berlin Heidelberg New York, 2001.
7. Browne, S., Zeigler, J., and Shepherd, J., "Numerical Solution Methods for Shock and Detonation Jump Conditions," Tech. Rep. FM2006-006, Graduate Aeronautical Laboratories California Institute of Technology, February 2008.